Cell

GroEL1: A Dedicated Chaperone Involved in Mycolic Acid Biosynthesis during Biofilm Formation in Mycobacteria

Anil Ojha,[1] Mridula Anand,[1] Apoorva Bhatt,[2] Laurent Kremer,[3] William R. Jacobs, Jr.,[2] and Graham F. Hatfull[1,*]
[1] Pittsburgh Bacteriophage Institute, Department of Biological Sciences, University of Pittsburgh, Pittsburgh, PA 15260, USA
[2] Howard Hughes Medical Institute, Albert Einstein College of Medicine, 1300 Morris Park Avenue, Bronx, NY 10461, USA
[3] Laboratoire de Dynamique Moléculaire des Interactions Membranaires, CNRS UMR 5539, Université de Montpellier II, Place Eugène Bataillon, 34095 Montpellier Cedex 05, France
*Contact: gfh@pitt.edu
DOI 10.1016/j.cell.2005.09.012

SUMMARY

Mycobacteria are unusual in encoding two GroEL paralogs, GroEL1 and GroEL2. GroEL2 is essential—presumably providing the housekeeping chaperone functions—while *groEL1* is nonessential, contains the *attB* site for phage Bxb1 integration, and encodes a putative chaperone with unusual structural features. Inactivation of the *Mycobacterium smegmatis groEL1* gene by phage Bxb1 integration allows normal planktonic growth but prevents the formation of mature biofilms. GroEL1 modulates synthesis of mycolates—long-chain fatty acid components of the mycobacterial cell wall—specifically during biofilm formation and physically associates with KasA, a key component of the type II Fatty Acid Synthase involved in mycolic acid synthesis. Biofilm formation is associated with elevated synthesis of short-chain (C_{56}–C_{68}) fatty acids, and strains with altered mycolate profiles—including an InhA mutant resistant to the antituberculosis drug isoniazid and a strain overexpressing KasA—are defective in biofilm formation.

INTRODUCTION

Biofilms are surface bound communities of microbial cells found in oligotrophic environments and are strongly implicated in bacterial virulence (Hall-Stoodley et al., 2004; Hall-Stoodley and Stoodley, 2005). Among human bacterial pathogens, the biofilms of *Pseudomonas aeruginosa*, *Haemophilus influenzae*, pathogenic *Esherichia coli*, *Vibrio cholerae,* and the Streptococci are some of the best studied (Kolter and Losick, 1998; Miller and Bassler, 2001; Fux et al., 2005; Reguera and Kolter, 2005), but the role of biofilms in the pathogenesis of *Mycobacterium tuberculosis* and *Mycobacterium leprae* (the causative agents of tuberculosis and leprosy, respectively) remains unclear. Several nontuberculous mycobacteria—including the saprophytic *Mycobacterium smegmatis* and the opportunistic pathogens *Mycobacterium avium* and *Mycobacterium chelonae*—have been shown to form biofilms (Carter et al., 2003; Primm et al., 2004), with implications for their extraordinary starvation survival (Nyka, 1974; Smeulders et al., 1999) and their resistance to antibiotics (Teng and Dick, 2003; Primm et al., 2004). Biofilms may also play a role in the pathogenesis of *Mycobacterium chelonae* and *Mycobacterium ulcerans,* the causative agents of chronic skin ulcers that also thrive in aquatic environments (Schulze-Robbecke et al., 1992; Kressel and Kidd, 2001; Marsollier et al., 2004a; Marsollier et al., 2004b), and the presence of biofilm-like structures in *M. ulcerans* infections of *Naucoris cimicoides* has been described (Marsollier et al., 2005). While the molecular events and regulatory circuitry in mycobacterial biofilm formation have yet to be elucidated, mutants altered in either undecaprenyl phosphokinase or glycopeptidolipid synthesis of the genetically facile *M. smegmatis* are defective in biofilm formation, reflecting the important role of cell wall biosynthesis in this process (Recht et al., 2000; Recht and Kolter, 2001; Rose et al., 2004). The long-chain (mycolic acids) fatty acids that constitute the characteristic mycobacterial cell walls are known to undergo dynamic structural fluctuations in response to changing environmental conditions (Baba et al., 1989; Yuan et al., 1998; Kremer et al., 2000a), but their response to biofilm formation has yet to be elucidated. Understanding the molecular events involved in the transition from planktonic growth to biofilm formation and the processes leading from surface attachment to generation of a mature biofilm is a central issue in bacterial physiology and has the potential to reveal novel interventions for bacterial infections.

The mycobacteria are unusual in encoding two forms of the Hsp60 chaperone GroEL (Kong et al., 1993), GroEL1 and GroEL2—with ~60% amino acid identity—and these were among the first mycobacterial genes identified using antibody screening of lambda gt11 libraries (Husson and

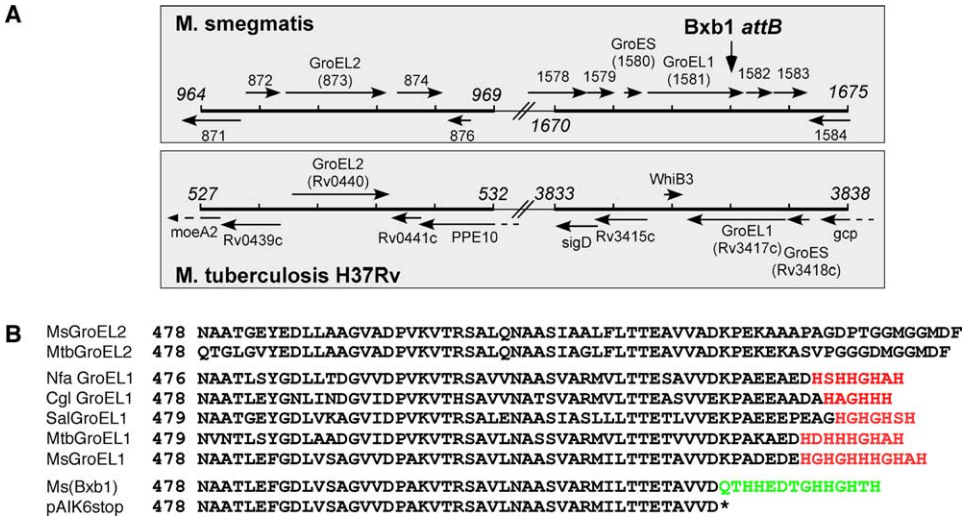

Figure 1. *M. smegmatis groEL1* Encodes an Unusual Hsp60 Chaperone

(A) Organization of the *groES*, *groEL1,* and *groEL2* genes in *M. smegmatis* (upper panel) and *M. tuberculosis* H37Rv (lower panel). *groEL1* is cotranscribed with *groES*, while *groEL2* is located more than 750 kbp away in both genomes; chromosomal locations (in italic type) are shown in kb. Phage Bxb1 integrates into the *attB* site in *groEL1* as shown.

(B) Mycobacterial GroEL1 proteins and their counterparts in other actinomycetes contain a histidine-rich C terminus (shown in red); GroEL1 proteins of *M. smegmatis* (Ms), *M. tuberculosis* (Mtb), *Nocardia farcinica* (Nfa), *Streptomyces albus* (Sab), and *Corynebacterium glutamicum* (Cgl) are shown, as are the GroEL2 proteins of *M. smegmatis* and *M. tuberculosis,* which contain glycine-methionine-rich C-terminal tails common to most GroEL proteins. Integration of either phage Bxb1 or the integration vector, pAlK6, generates a different C terminus (shown in green), and integration by plasmid pAlKstop makes a truncated protein.

Young, 1987; Young et al., 1988). Although the sequence differences are distributed throughout the lengths of the proteins, GroEL1 has a distinctive histidine-rich C terminus, while GroEL2 has a glycine–methionine-rich C terminus that is more typical of these chaperones (Figure 1B); *M. smegmatis* also encodes a third Hsp60 protein (SMEG1981) that is more distantly related to GroEL1 and GroEL2. The mycobacteria contain just a single *groES* gene which is transcriptionally fused to *groEL1* (Kong et al., 1993) (Figure 1A). In *Mycobacterium tuberculosis,* both GroEL proteins are upregulated during heat shock (Stewart et al., 2002), oxidative stress response (Dosanjh et al., 2005), and macrophage infection (Monahan et al., 2001), and they are implicated in the immune response to *M. tuberculosis* infection (Orme et al., 1993; Coates, 1996; Lewthwaite et al., 2001). The best studied member of the Hsp60 chaperones is that encoded by *E. coli*, which is composed of two 7-membered toroidal rings of GroEL acting in concert with its cochaperone, GroES (Braig et al., 1994; Xu et al., 1997; Sigler et al., 1998; Saibil, 2000). The central cavity of the protein provides an environment for folding newly synthesized, imported, and misfolded proteins (Hartl et al., 1992) and promotes folding of 10%–15% of cytosolic proteins (Ewalt et al., 1997; Houry et al., 1999). *E. coli* GroE also facilitates the assembly of multisubunit complexes, including viral capsids (Hendrix and Tsui, 1978; Fisher, 1998; Grimaud and Toussaint, 1998). The synthesis of *E. coli* GroE is induced upon exposure to stress (Herman and Gross, 2000) but is required for *E. coli* growth at all temperatures (Fayet et al., 1989).

For those bacteria—such as members of the α-proteobacteria, the cyanobacteria, and the actinomycetes—that contain multiple copies of *groEL* (Karlin and Brocchieri, 2000), it is unclear what roles are fulfilled by these genes. Presumably, one of the *groEL* genes provides the usual housekeeping chaperone functions exemplified by *E. coli* GroEL, and the additional copies either further elevate chaperone abundance, provide expression in response to specific environmental or stress conditions, or chaperone specific subsets of cellular protein substrates. Alternatively, they could perform some of the additional roles ascribed to Hsp60 proteins, such as intercellular signaling (Maguire et al., 2002) and transcriptional regulation (Guisbert et al., 2004). In *Sinorhizobium meliloti,* one of the five GroEL paralogs, GroEL, is nonessential for growth and influences the folding and assembly of NodD (Ogawa and Long, 1995). However, it is noteworthy that the unusual histidine-rich C termini of the secondary GroEL proteins in the actinomycetes are not found in either the cyanobacteria or the α-proteobacteria.

Mycobacteriophage Bxb1 is a temperate phage of *M. smegmatis* that integrates into an *attB* site located within the 3′ end of the *groEL1* gene (Ghosh et al., 2003; Kim et al., 2003). We show here that Bxb1 lysogens are defective in biofilm formation as a direct consequence of inactivation of the *groEL1* gene. Loss of GroEL1 function does not affect planktonic growth or surface attachment but specifically interferes with biofilm maturation. The behavior of a *groEL1* knockout mutant reveals that mycolic acid synthesis is regulated during biofilm formation and that GroEL1 physically

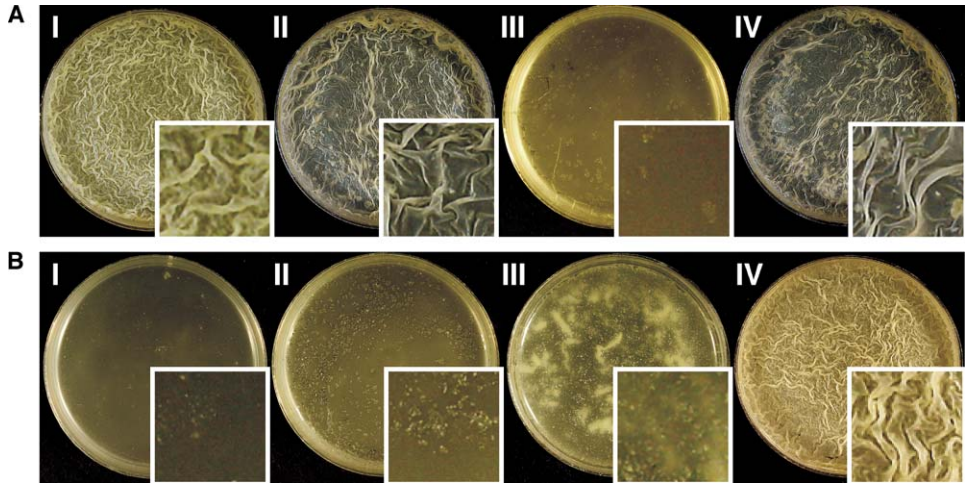

Figure 2. GroEL1 Is Required for Biofilm Formation

(A) Bxb1 lysogens are defective in biofilm formation. *M. smegmatis* mc^{2}155 (I) and lysogens of phages L5 (II), Bxb1 (III), and Che12 (IV) were grown on a liquid surface at 30ºC for 7 days; insets show 4×-magnified portions of the biofilm.

(B) Interruption of the *M. smegmatis groEL1* gene by integration of the Bxb1 integration-proficient plasmid vector, pAIK6 (I), integration of the plasmid pAIK-stop, which terminates 18 residues from the C terminus of GroEL1 (II), or by deletion (III) results in loss of biofilm formation; complementation with wild-type *groEL1* restores biofilm formation (IV).

associates with the FAS-II component, KasA, to facilitate this regulation. The central role of mycolate synthesis in biofilm formation is illustrated by the observations that short-chain mycolates are upregulated during biofilm formation and that mutants defective in the type II fatty acid Synthase (FAS-II) components KasB and InhA—including those conferring resistance to the major antituberculosis drug isoniazid—are defective in biofilm maturation.

RESULTS

Bxb1 Lysogens Are Defective in Biofilm Formation through Inactivation of GroEL1

Mycobacteriophage Bxb1 is a temperate phage of *M. smegmatis* and forms lysogens in which the Bxb1 prophage is integrated at an *attB* attachment site located within the extreme 3′ end of the *groEL1* gene (Mediavilla et al., 2000; Kim et al., 2003) (Figure 1A); integration results in substitution of the C-terminal 18 residues (N-KPADEDEHGHGHHH GHAH) with 14 phage-encoded residues (N-QTHHEDTGH HGHTH) (Figure 1B). Bxb1 lysogens show normal growth patterns on agar plates and in planktonic growth, suggesting that either the *groEL1* gene is nonessential or that the recombinant gene in Bxb1 lysogens is fully functional (Kim et al., 2003). However, while investigating the interactions of phages with bacterial biofilms, we observed that Bxb1 lysogens exhibit a strong defect in biofilm formation (Figure 2A). Transformation with an integration-proficient plasmid (Figure 2B-I) that lacks all of the Bxb1 genome except the integration apparatus, or a plasmid derivative (pAIK6stop) that prematurely terminates the *groEL1* gene 18 codons from the 3′ end (Figure 1B-II), generates a similar biofilm defect. Complete removal of the *groEL1* gene also results in loss of biofilm formation (Figure 2B-III) with little or no effect on planktonic growth (Figure S1), and the defect is complemented by reintroduction of the *groEL1* gene (Figure 2B-IV). In contrast, *groEL2* is an essential gene in *M. smegmatis* (Figure S2) and also has recently been reported to be essential in *Corynebacterium glutamicum,* whereas GroEL1 is dispensable (Barreiro et al., 2005). As expected, lysogens of mycobacteriophages L5 and Che12, which do not integrate into the *groEL1* gene, are not defective in biofilm formation (Figure 2A). Altogether, these results indicate that *groEL1* is specifically required for growth of *M. smegmatis* biofilms under the conditions tested. It is unclear what—if any—selective advantage is conferred upon Bxb1 lysogens by this unusual phenotype.

GroEL1 Is Required for Biofilm Maturation, Not for Attachment

Development of a mature *M. smegmatis* pellicle-like biofilm at a liquid-air interface takes 4–7 days at 30ºC (Recht et al., 2000; Branda et al., 2005). For the first 3 days following inoculation, *M. smegmatis* cells grow at the surface to form a uniform thin film, and at day 4 the appearance of surface texture, including ridges and troughs, begins. (Figure 3A). This appearance is more obvious by day 5, and by day 7 small structures reminiscent of microcolonies also appear (Figure 3A); after day 7 there is little further change in biofilm appearance (data not shown). The Δ*groEL1* mutant behaves similarly to its mc^{2}155 parent up to day 3 but fails to generate the characteristic surface texture during longer periods of incubation (Figure 3A). Determination of colony forming units (cfu) indicates that growth of the Δ*groEL1* mutant slows considerably after 3 days under these conditions (Figure 3D). *M. smegmatis* thus proceeds through defined stages of

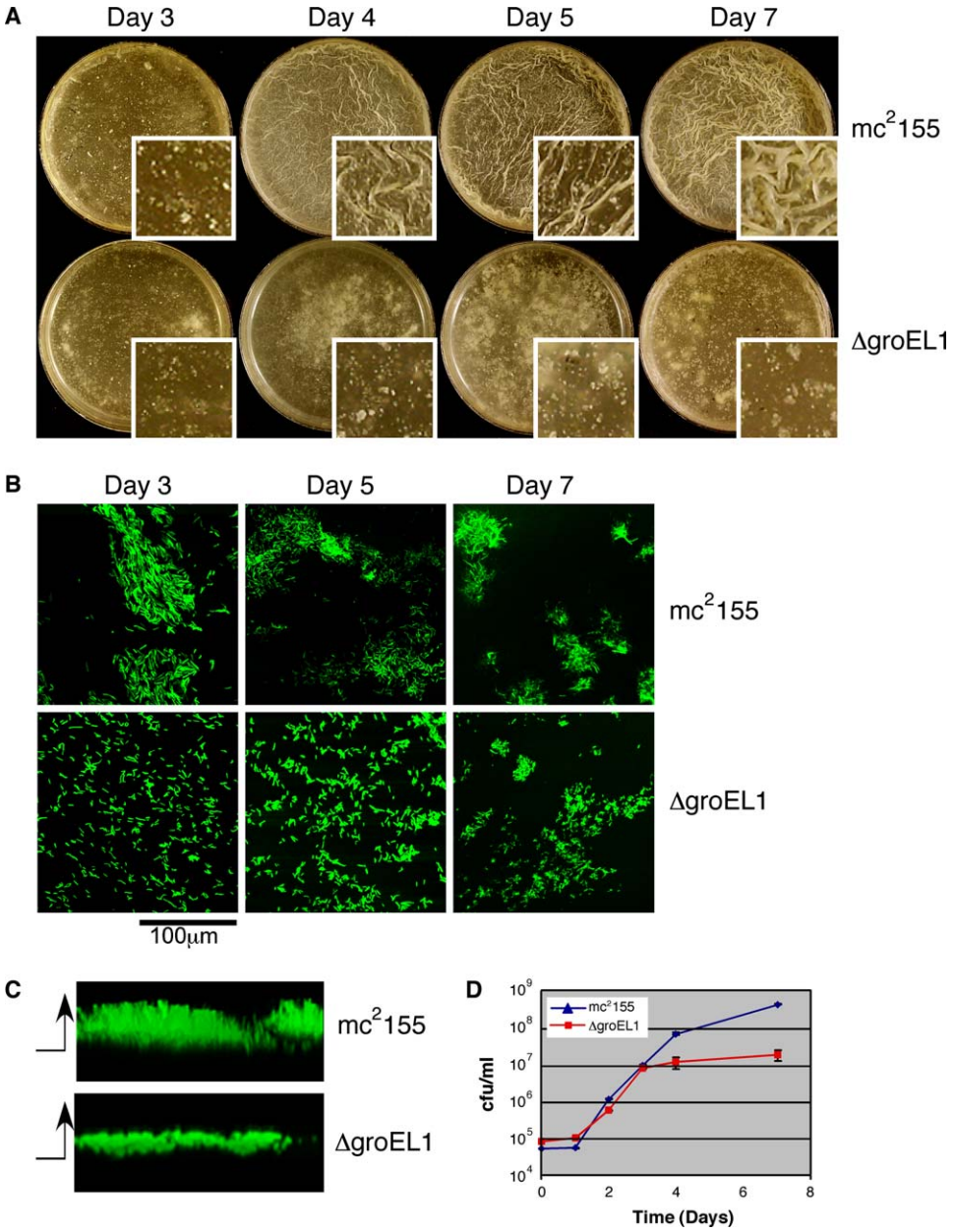

Figure 3. *M. smegmatis* GroEL1 Is Required for Biofilm Maturation but Not for Attachment

(A) Time course of biofilm development at a liquid-air surface. Dishes containing liquid growth medium were inoculated with either *M. smegmatis* mc^{2}155 or a Δ*groEL1* mutant, and biofilms were allowed to develop for 7 days at 30ºC. At day 3, *M. smegmatis* mc^{2}155 forms a thin film across the surface of the medium, and by day 4 it begins to form a textured mature biofilm that continues to develop until day 7. The Δ*groEL1* mutant forms a similar film to the parent strain mc^{2}155 by day 3 but does not develop further.

(B and C) Attachment of *M. smegmatis* mc^{2}155 and Δ*groEL1* mutant to a PVC surface. Strains were transformed with a GFP-expressing plasmid, grown on PVC slides for 7 days, and viewed by fluorescence microscopy. The Δ*groEL1* cells attach as a monolayer to the PVC but do not form a mature biofilm, as further illustrated in the Z sections derived from confocal microscopy of the 7-day slides as shown in (C); horizontal lines indicate the approximate position of the surface, and vertical arrows show the direction of biofilm growth away from the surface.

(D) Growth of *M. smegmatis* in biofilm dishes. Following inoculation of medium as described in (A), viable cell counts were determined at various times, showing that Δ*groEL1* growth is compromised after 3 days of incubation.

biofilm development, and GroEL1 is specifically required for complete growth and biofilm maturation but not for initial growth at the liquid-air interface. To determine if GroEL1 is required for surface attachment, we used an assay in which GFP-expressing *M. smegmatis* biofilms are grown on a PVC surface (O'Toole et al., 1999) and visualized by fluorescence

microscopy. The Δ*groEL1* mutant cells are able to attach to the surface but—in contrast to its mc^{2}155 parent—grow in a dispersed manner (Figure 3B), and an optical sectioning along the Z axis by confocal microscopy shows that the Δ*groEL1* mutant forms a thin layer of cells across the PVC surface rather than the thicker textured wild-type biofilm (Figure 3C). This maturation defect of the Δ*groEL1* mutant is distinct from the attachment and spreading phenotypes of *M. smegmatis* mutants defective in either glycopeptidolipid synthesis genes or in undecaprenyl kinase (Recht et al., 2000; Rose et al., 2004).

GroEL1 Is Required for Regulation of Mycolate Biosynthesis in Biofilm Maturation

To examine the specific role of GroEL1, we compared the proteomic profiles of the Δ*groEL1* mutant and its mc^{2}155 parent by 2D-PAGE, using cells harvested from stationary phase cultures (Figure 4A). The profiles appear largely similar, although a small number of protein species are at reproducibly lower levels in the mutant relative to mc^{2}155. Two spots were excised from the mc^{2}155 gel and identified as KasA and KasB, two related β-ketoacyl-acyl carrier protein (ACP) synthases that are components of the FAS-II complex active in mycolic acid biosynthesis (Kremer et al., 2000b; Schaeffer et al., 2001; Kremer et al., 2002a; Slayden and Barry, 2002). During logarithmic planktonic growth of *M. smegmatis*, there is little difference in the total KasA/KasB levels between the Δ*groEL1* mutant and mc^{2}155 strains (Figure 4B), yet in early stationary phase growth there is a change in the relative abundance of the two isoforms of KasA separable by 2D-PAGE (Figure 4C). The molecular basis for the difference in mobility of these two KasA isoforms is unknown, although this change accounts for the differences observed in the proteomic comparison shown in Figure 4A; the weakly abundant 80 kDa species seen in Figure 4B likely corresponds to the previously reported 80 kDa covalent complex—containing KasA and the mycobacterial acyl carrier protein AcpM—that increases in abundance following treatment with InhA-inhibitory drugs (Mdluli et al., 1998; Kremer et al., 2003). Interestingly, there is a marked reduction in KasA and KasB levels—especially of KasA—in cells collected from Δ*groEL1* biofilm cultures (Figure 4C) relative to those of mc^{2}155, and the reduction begins between day 3 and day 4 of biofilm growth (Figure 4D), corresponding to the transition to biofilm maturation that the Δ*groEL1* mutant is defective in. However, the levels of the enoyl-ACP reductase, InhA, remain constant (data not shown). Restoration of KasA/KasB levels similar to those found in the mc^{2}155 strain was achieved in the Δ*groEL1* complemented strain (Figure 4D). Moreover, there is a substantial reduction in the level of mycolate synthesis in the Δ*groEL1* mutant during biofilm development, compared to its wild-type parent (Figure 4E). When taken together, these data suggest that the transition to formation of mature biofilms requires changes in mycolate synthesis and that GroEL1 plays a key role in these regulatory events.

Since many of the component subunits of the FAS-II enzymes have been shown to physically interact—including KasA and InhA (Veyron-Churlet et al., 2004)—GroEL1 could conceivably play a role in the assembly of FAS-II complexes during biofilm maturation, and an assembly failure in the mutant results in turnover of the unassembled FAS-II components. However, this raises questions as to whether GroEL1 is indeed directly involved in the regulation of mycolic acid biosynthesis and what makes GroEL1 functionally distinct from its GroEL2 counterpart.

GroEL1 Physically Associates with KasA during Biofilm Formation

Since Bxb1 integration alters the extreme 3′ end of the *groEL1* gene (Figure 1) but results in a phenotype consistent with complete inactivation of GroEL1 function, the histidine-rich terminal 18 residues appear to be important for GroEL1 function. During purification of proteins from *M. smegmatis*, we serendipitously observed that GroEL1 binds to an Ni-affinity matrix and elutes with 75 mM imidazole. The binding is likely to be mediated by the extreme C terminus of the protein since removal of the last 18 amino acids (by integration of pAlK6stop; see Figure 1) destroys metal binding (Figure 5A). Reconstitution of the recombinant GroEL1 protein corresponding to that generated by Bxb1 integration (by integration of plasmid pAlK6; see Figure 1) does not restore Ni binding (Figure 5A), showing that this is a sequence-dependent property of GroEL1 and not simply a reflection of the abundance of histidine residues.

The metal binding property of GroEL1 is a particularly useful attribute for addressing the structure and function of the enzyme. In particular, Western blot analysis of the purified GroEL1 protein using two antisera with differential preferences for GroEL1 and GroEL2 (Figure 5B) shows that GroEL2 does not copurify with GroEL1. GroEL1 therefore does not heteromultimerize with GroEL2 and is thus both functionally and structurally distinct from its Hsp60 counterpart. We do not know what metal—if any—is bound by GroEL1 in vivo, although we note that growth of *M. smegmatis* biofilms requires relatively high concentrations of iron, and withdrawal of the iron supplement leads to inhibition of biofilm maturation while having little effect on planktonic growth (Figure S3). Since loss of GroEL1 and iron withdrawal result in similar phenotypes, an intriguing possibility is that GroEL1 binds iron and that iron withdrawal leads to inactivation of GroEL1. However, we note that other biofilm-forming bacteria such as *P. aeruginosa* also require iron for biofilm growth (Singh et al., 2002) but do not encode a GroEL1-like protein. The small GroE subunit (GroES) of *M. leprae* has also been shown to bind divalent transition metals Ni^{2+}, Mn^{2+}, and Zn^{2+} (Taneja and Mande, 2001).

The changes in the FAS-II component KasA and in mycolate synthesis that result from deletion of *groEL1* (Figure 4) suggest the possibility that the mycolate profile of *M. smegmatis* is fundamentally different in biofilm formation and planktonic growth and that GroEL1 could interact directly with KasA to facilitate the regulation. Using the Ni binding properties of GroEL1, we observed that only low levels of KasA copurify with GroEL1 using extracts of planktonically grown cells but that the level increases approximately

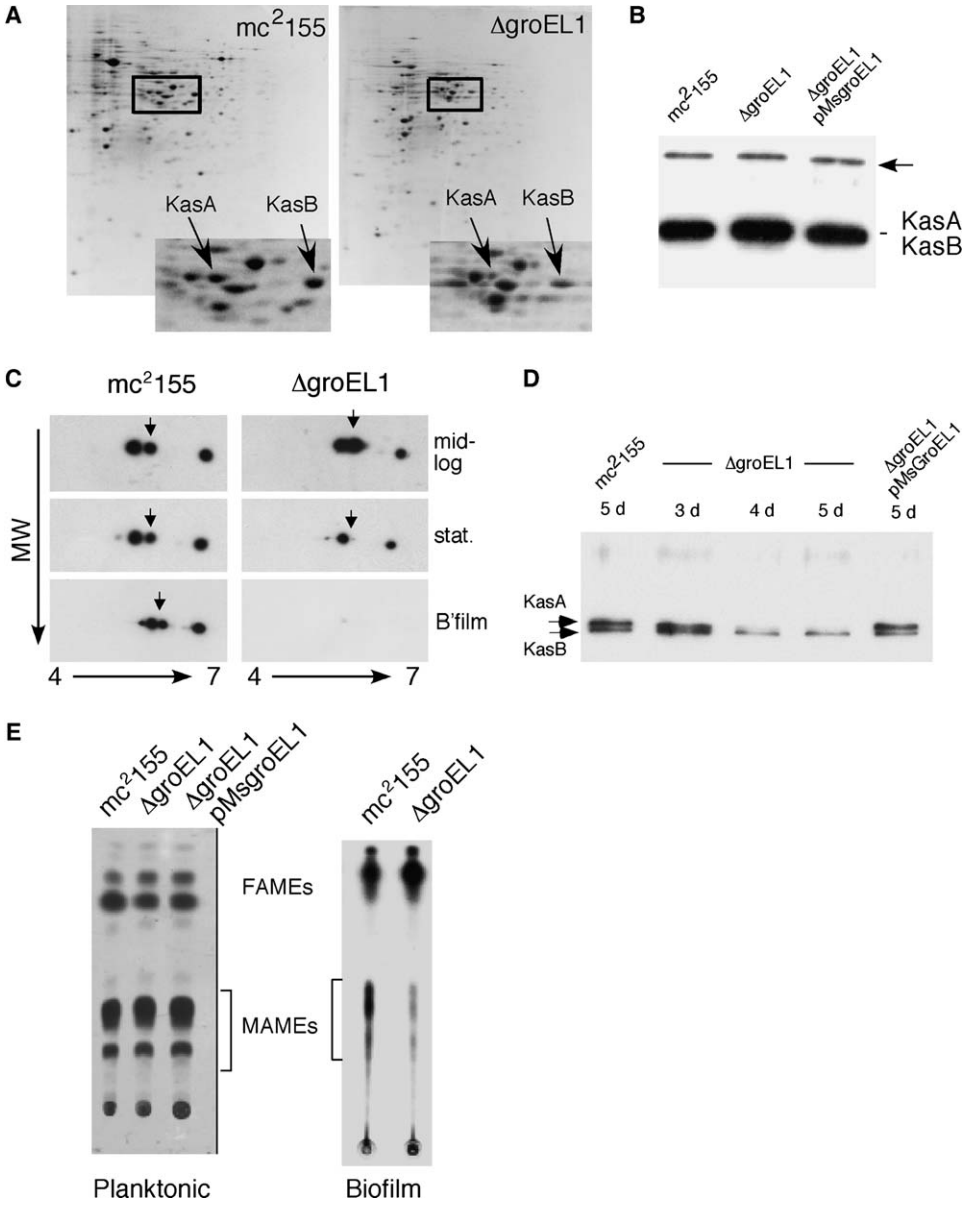

Figure 4. GroEL1 Is Required for Mycolic Acid Biosynthesis during Biofilm Formation

(A) 2D-PAGE reveals two protein species present at reduced levels in the Δ*groEL1* mutant relative to its mc^{2}155 parent in stationary phase cells; identities of the protein spots were determined by either N-terminal sequencing or mass spectometry.

(B) Western blot analysis of total KasA/KasB levels during logarithmic planktonically grown cells reveals similar levels in Δ*groEL1*, mc^{2}155 parent, and complemented strains. The antibody recognizes both KasA and KasB, which migrate similarly, as well as the slowly migrating 80 kDa complex (indicated by arrow) that also contains AcpM (Mdluli et al., 1998).

(C) Western blot analysis of KasA/KasB separated by 2D-PAGE shows a single KasB and two KasA protein species. The level of the more basic of the two KasA spots (shown by arrow) varies under different growth conditions, but all KasA/KasB species are reduced in the Δ*groEL1* mutant after 7 days of biofilm growth.

(D) The reduction of KasA and KasB in the Δ*groEL1* mutant begins at day 4, correlating with the cessation of growth and inability to transition to biofilm maturation.

(E) Thin-layer chromatography of radiolabeled fatty acid methyl esters (FAMEs) and mycolic acid methyl esters (MAMEs) shows that the biosynthesis of all mycolic acid subclasses (α, α′, and epoxy) is dramatically reduced in the Δ*groEL1* mutant during biofilm maturation but not in planktonic cultures.

15-fold in biofilm-grown cells (Figure 5C); 2D-PAGE shows that predominantly only one of the KasA isoforms (and not KasB) copurifies (data not shown). The enoyl-ACP reductase InhA was not found associated with GroEL1 in either the planktonic or biofilm samples (data not shown). It is noteworthy that the enhancement of GroEL1-KasA association does

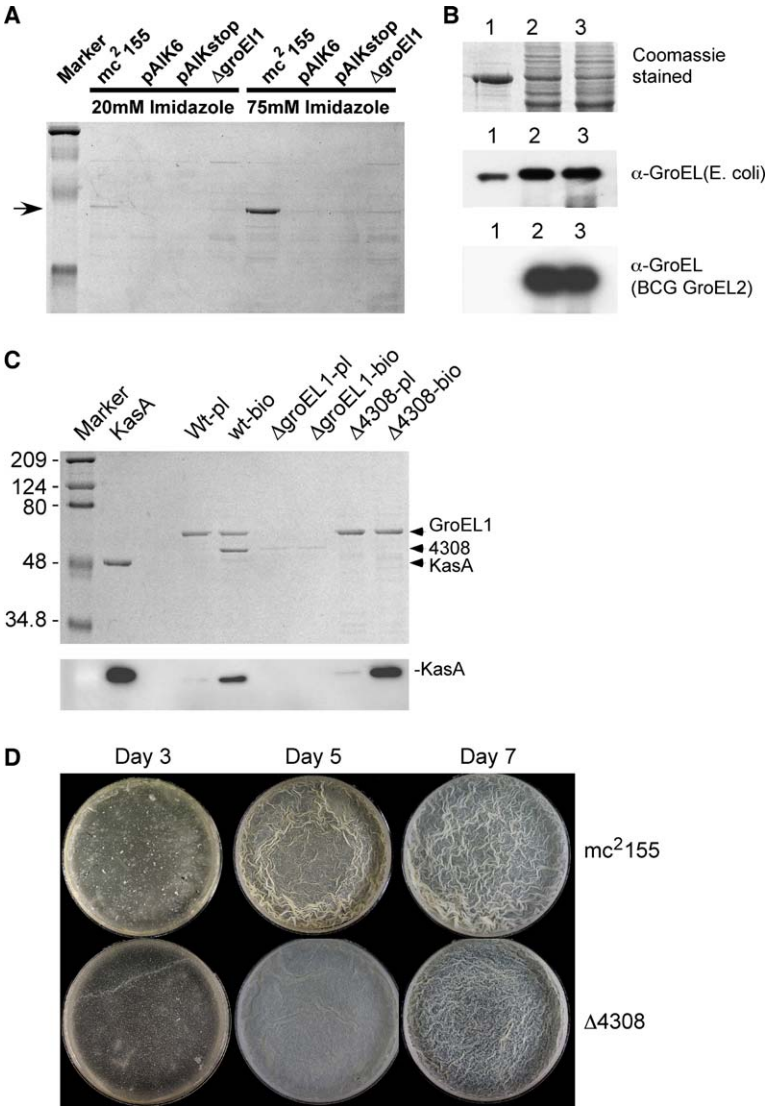

Figure 5. Physical Association of GroEL1 and KasA

(A) *M. smegmatis* GroEL1 binds to Nickel-affinity columns. Extracts of *M. smegmatis* mc^{2}155 (lanes 1), Δ*groEL1* mutant (lanes 2), and a pAIK6stop recombinant were bound to an Ni-affinity column and proteins eluted with either 20 mM or 75 mM imidazole as indicated. The position of GroEL1 is indicated with an arrow.

(B) SDS-PAGE was used to separate either GroEL1 eluted from an Ni-affinity column (lanes 1), a total extract from *M. smegmatis* mc^{2}155 (lanes 2), or an extract from a Δ*groEL1* mutant (lanes 3). Proteins were transferred to a membrane and blotted with either polyclonal antibodies raised against *E. coli* GroEL or monoclonal antibodies raised against GroEL2 of bacilli Calmette Guerin (BCG, as indicated). Coomassie blue–stained proteins are shown in upper panel. Both antibodies recognize a 60 kDa protein in the Δ*groEL1* strain, showing that they both recognize GroEL2. However, only the *E. coli* antibody recognizes the protein eluted from the Ni-column, showing both that the BCG-GroEL2 monoclonal antibody does not recognize GroEL1 and that the protein eluted from the Ni-column contains GroEL1 and not GroEL2.

(C) Interaction between GroEL1 and KasA in planktonic and biofilm cells. Extracts from planktonic (pl) or biofilm (bio) samples from *M. smegmatis* mc^{2}155, Δ*groEL1,* and Δ*smeg4308* were passed over an Ni-affinity column, and the proteins were eluted with 75 mM imidazole and separated by SDS-PAGE. Lane 2 contains 2 μg of purified KasA protein. The upper panel shows Coomassie blue–stained proteins, whereas the lower panel shows a Western blot of the same samples (and 20 ng of purified KasA) using anti-KasA serum.

(D) A Δ*smeg4308* mutant is defective in biofilm formation. Biofilms were grown as in Figure 3, and the Δ*smeg4308* mutant shows a mild defect such that mature biofilm features are not seen at day 5 but begin to appear at day 7.

not result from changes in the total abundance of either protein, and microarray experiments show that there is no significant change in the expression of either protein during biofilm development (data not shown).

Although the amount of KasA associating with GroEL1 is substantially enhanced in biofilm-grown cells, staining of the associated proteins shows that the amount of KasA is substoichiometric to the amount of GroEL1 (Figure 5C). However, an additional protein is present in the biofilm samples in equivalent abundance to GroEL1, though it is absent from planktonically grown cells. N-terminal sequencing reveals this to be SMEG4308 (predicted molecular weight of 55 kDa), a protein of unknown function which is composed of a thioredoxin reductase-like domain and a methylase domain related to that involved in cyclopropyl fatty acid synthesis. The absence of SMEG4308 in the planktonic sample can be accounted for by regulation of gene expression (rather than changes in GroEL1 association) since microarray experiments show that SMEG4308 is one of the most highly upregulated genes (>50-fold) in the transition from planktonic growth to biofilms (data not shown). Since SMEG4308 could conceivably mediate the association of KasA with GroEL1, we constructed a mutant lacking the *smeg4308* gene. The loss of SMEG4308 does not affect the change in association of GroEL1 and KasA (Figure 5C). Therefore, it seems likely that the enhanced GroEL1-KasA association in biofilms results either from posttranslational changes in the proteins or from differences in cellular localization. Interestingly, the Δ*smeg4308* mutant exhibits a defect in biofilm formation—albeit in a significantly milder form than observed with the Δ*groEL1* mutant—indicating that this GroEL1-associated protein is also involved in biofilm formation (Figure 5D).

Changes in the Mycolic Acid Profile during Biofilm Formation

The properties of the Δ*groEL1* mutant suggest that there are distinct differences in mycolate synthesis in planktonic and

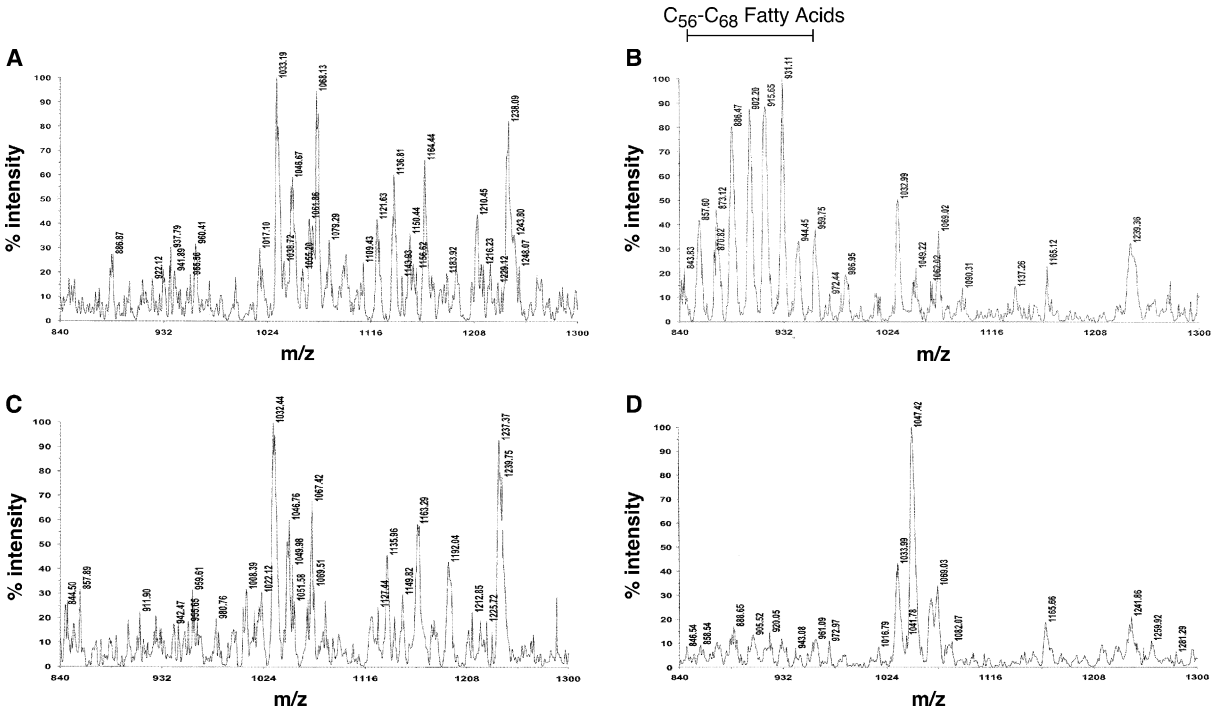

Figure 6. The Ratio of Short- to Long-Chain Mycolates Increases during Biofilm Formation

(A, B, C, and D) Total mycolates were extracted from *M. smegmatis* mc^{2}155 cells (A and B) or ΔgroEL1 (C and D), growing in either log-phase planktonic (A and C) or 4-day biofilm (B and D) conditions and analyzed by MALDI-TOF mass spectrometry. Short-chain fatty acids (C_{56}–C_{68}) are seen as a series of peaks with masses ranging from 857 to 961.

biofilm grown cells that are not readily evident from analysis by TLC (Figure 4E and data not shown) but may be relevant to biofilm formation. To test this, total mycolates were extracted from planktonic and biofilm-grown cells and examined by mass spectrometry. A substantial increase in the prevalence of shorter chain mycolic acids—with masses corresponding to C_{56}–C_{68} chains or their derivatives—in the biofilm sample was observed (Figure 6). The individual species within this mass range correspond to both odd- and even-numbered fatty acid chains (i.e., differing by 14 mass units), which may correspond to two interleafed series of fatty acids, both differing in chain lengths of two carbons (deriving from the incorporation of malony-CoA by FAS-II), but one with an additional modification (such as methylation). However, we note that SMEG4308—which contains a methylase domain—is not responsible for such a modification since cells harvested from Δ*smeg4308* cells grown under biofilm conditions show a similar series of C_{56}–C_{68} mycolates (data not shown). It is noteworthy that this collection of fatty acids is more complex than the previously described α′-mycolates—which predominantly differ by mass units of 28 (Laval et al., 2001)—although these may be present within this series; alternatively, these C_{56}–C_{68} fatty acids may correspond to meromycolate precursors of α-mycolates. Although the total mycolate content is greatly reduced in the *ΔgroEL1* mutant (Figure 4E), harvesting cells from a total of ten dishes provided enough material for analysis by mass spectrometry, and the profiles show a clear lack of induction of the C_{56}–C_{68} chains (Figure 6). These data are consistent with the interpretation that GroEL1 is required for the induction of the C_{56}–C_{68} fatty acids and that failure to induce them results in the inability to form mature biofilms.

Mutants Defective in Mycolate Biosynthesis Are Also Defective in Biofilm Maturation

The significant changes in the mycolate profile that occur during biofilm formation suggest the possibility that mutants affected in mycolate biosynthetic enzymes may also exhibit biofilm defects. An InhA^{ts} mutant—that is temperature-sensitive for growth but highly resistant to isoniazid (MIC > 100 μg/ml) at the permissive temperature—has been previously reported to have differences in its mycolate profile (including a reduction in the α′-mycolates) (Vilcheze et al., 2000); interestingly, it also shows a significant defect in biofilm maturation at the permissive temperature while growing normally planktonically (Figure S1). While this phenotype could result directly from a change in InhA activity, it is also possible that the biofilm defect results from secondary consequences of the InhA^{ts} mutation, and it is known that KasA is upregulated in this strain (Kremer et al., 2003). We therefore also examined a strain in which KasA is overexpressed from an extrachromosomal plasmid (pMV261:KasA) and observed that while it is capable of forming a mature biofilm, it is delayed in doing so, and there are no mature biofilm features after either 4 or 5 days of growth (Figure 7B). Interestingly, the same strain has been shown previously to have an

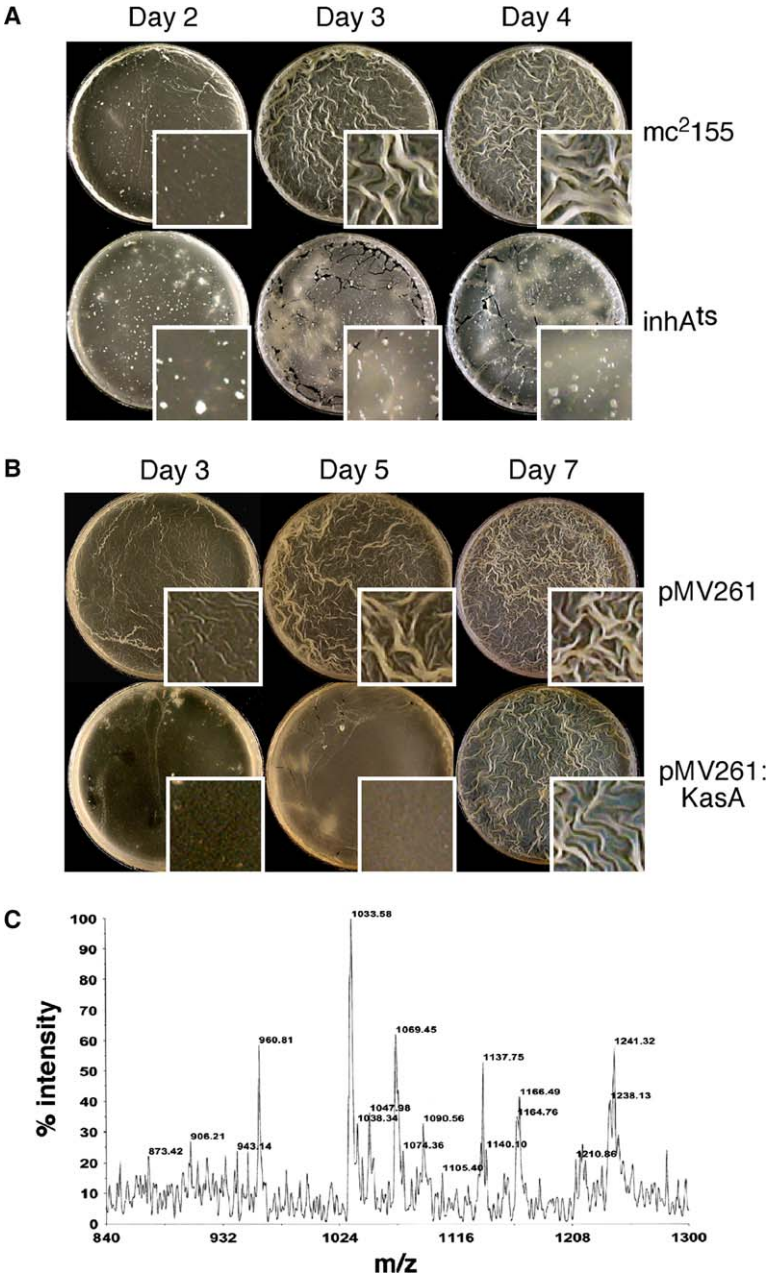

Figure 7. *M. smegmatis* Mutants Altered in Mycolic Acid Biosynthesis Are Also Defective in Biofilm Formation

(A) An *inhA*^{ts} strain is defective in biofilm maturation at 33ºC and forms only thin films reminiscent of the Δ*groEL1* mutant (Figure 2B); the mutant grows similarly to mc^{2}155 in planktonic growth (Figure S1). The biofilm defect is also observed at 30ºC, but with a milder phenotype, and at 37ºC there is significant impairment of planktonic growth (data not shown).

(B) Overexpression of KasA retards biofilm maturation, and a strain carrying a plasmid overexpressing KasA from the *hsp60* promoter (pMV261:kasA) is slower in biofilm maturation than a vector-containing strain (pMV261). Both strains grow at similar rates planktonically (Figure S1).

(C) MALDI-TOF mass spectrometry of mycolates from 4-day biofilm cultures of mc^{2}155pMV261:KasA showing reduced levels of C_{56}–C_{68} fatty acids.

altered mycolate profile, including a reduction of α′-mycolates (Kremer et al., 2002a). When we examined the fatty acids from a 4-day grown biofilm of the KasA-overexpressing strain, we observed no induction of the C_{56}–C_{68} fatty acids (Figure 7C), in marked contrast to a wild-type biofilm sample harvested at the same time (Figure 6B). The mycolates of the InhA^{ts} strain from a day-4 biofilm were also examined (Figure S4), and while these do induce the C_{56}–C_{68} chains, the entire mycolate profile is different, complicating any correlation with the biofilm phenotype.

Taken together, these observations support a model in which the transition from early biofilm formation to maturation involves a GroEL1-dependent switch in mycolate synthesis characterized by elevated synthesis of C_{56}-C_{68} fatty acids, representing either short-chain mycolates or meromycolate precursors. We propose that the role of GroEL1 in this switch involves physical association with KasA and SMEG4308 and that loss of GroEL1 results not only in the inability to induce synthesis of the C_{56}–C_{68} fatty acids but in destabilization of KasA and a consequent reduction in all mycolate synthesis. What triggers the switch is unclear but probably involves either chemical or physical cellular communication in a density-dependent manner. In this model, we suggest that the level of KasA plays a role in the timing of the transition of mycolate synthesis such that overexpression of KasA causes a significant delay in the transition

(Figure 7C), and at times when wild-type cells are forming both mature biofilms and synthesizing C_{56}–C_{68} mycolates, the KasA-overexpressing strain does neither. One intriguing possibility is that the mycolate switch requires a GroEL1-dependent conversion of one KasA isoform to another and that this conversion takes longer if there are great amounts of the initial form present. However, elucidating the molecular machinery involved is confounded by our rather poor understanding of many aspects of mycolate synthesis—such as why α′-mycolates are decreased when KasA is overexpressed (Kremer et al., 2002a) and why they are resistant to INH (Kremer et al., 2003). These questions remain unanswered. Finally, we note that inactivation of *kasB* also leads to a delay in biofilm maturation (data not shown), perhaps reflecting its strong association with KasA (Veyron-Churlet et al., 2004).

DISCUSSION

The behaviors of the Bxb1 lysogen and the Δ*groEL1* mutant reveal an interesting and unsuspected role of the unusual chaperone, GroEL1, in the synthesis of mycolic acids, performing a regulatory function that is not required in planktonic growth but is needed for biofilm maturation. Whether GroEL1 is required for other metabolic processes is unclear, although we note that there are few obvious changes in the 2D-PAGE profile resulting from GroEL1 removal (Figure 4), and the most noticeable differences between the proteins that copurify with GroEL1 from biofilms and planktonically grown cells involve KasA and SMEG4308 (Figure 5), both of which are implicated in biofilm formation. As in other bacterial systems, biofilm formation of *M. smegmatis* involves both up- and downregulation of the transcriptome (Beloin and Ghigo, 2005; A.O. and G.F.H., unpublished data), but—with the notable exception of SMEG4308—it is not clear whether the functions of these proteins are influenced by GroEL1. Interestingly, the transcription of neither GroEL1 nor any of the FAS-II subunits is substantially upregulated during biofilm formation (A.O. and G.F.H., unpublished), suggesting that the action of GroEL1 is primarily posttranslational, involving its physical association with KasA and SMEG4308. A similar form of regulation may also occur in *Nocardia* and *Corynebacterium,* two genera that have been reported to make biofilms—both of which contain a GroEL1 similar to that in the mycobacteria (Figure 1B)—and have mycolic acids in their cell walls.

Since *M. tuberculosis* encodes a similar GroEL1 protein to that in *M. smegmatis*, the question arises as to the possible role of GroEL1 in *M. tuberculosis* pathogenesis. Since it is known that *M. tuberculosis* mutants defective in mycolate synthesis have attenuated phenotypes (Dubnau et al., 2000; Glickman et al., 2000), it seems probable that an *M. tuberculosis* Δ*groEL1* mutant will also be defective in virulence. While planktonic *M. tuberculosis* does not form α′-mycolates, we cannot rule out that a similar series of C_{56}–C_{68} mycolates or meromycolates is induced under appropriate conditions, and it has been shown previously that other aspects of mycolic acid structure change dynamically in response to different environments (Kremer et al., 2000a). The possibility of biofilm formation during *M. tuberculosis* infection of mammalian cells remains an unresolved question but could give rise to drug-tolerant organisms that persist for long durations of drug treatment. A Δ*groEL1* mutant of *M. tuberculosis* should provide a powerful tool for addressing these questions.

EXPERIMENTAL PROCEDURES

Bacterial Strains and Growth Media

M. smegmatis mc^2155 was used as the parent (wild-type) strain. All strains were maintained in either 7H10 agar or 7H9 + ADC with appropriate antibiotics (Δ*groEL1*—150 μg/ml hygromycin; Δ*groEL1*pMsgroEL1—150 μg/ml hygromycin and 25 μg/ml kanamycin; Δ*kasB*—150 μg/ml hygromycin; $inhA^{ts}$—150 μg/ml hygromycin and 25 μg/ml isoniazid). For biofilm cultures grown on liquid medium, 10 ml of biofilm medium—a modified version of M63 (Recht and Kolter, 2001)—in a 60 × 15 mm^2 polystyrene Petri dish was inoculated with 10 μl of a saturated culture and incubated at 30ºC (unless otherwise stated) without disturbance. To determine the numbers of viable bacteria, biofilm cultures were incubated with tween-80 (final concentration, 0.05%) for 30 min at 25ºC, cells were collected by centrifugation, disrupted with 0.5 mm glass beads in a mini bead beater (Bio-spec) for 30 s at maximum speed, and plated onto solid media. Colony-forming units (cfu) were measured as the mean of three independent observations. For growth of biofilm cultures on PVC coverslips, 10 μl of saturated cultures of either mc^2155 or *ΔgroEL1*—transformed with a plasmid pJL37GFP containing GFP under the BCG *hsp60* promoter—was inoculated into 6 ml of biofilm medium in a 50 ml conical tube with a PVC coverslip partially submerged in the medium. Coverslips were taken out at time intervals, washed several times with water, mounted on a microscope slide, and viewed under a Confocal Scanning Laser Microscope (Nikon, Bio-Rad). For planktonic growth, cultures were inoculated at the same dilution in biofilm medium containing 0.05% tween-80 and incubated at 30ºC on a shaker platform maintained at 200 rpm.

Plasmids

Plasmids pMsGroEL1 and pMsGroEL2 contain *M. smegmatis groEL1* and *groEL2,* respectively, in vector pJL37 (Lewis and Hatfull, 2000), although the resident *hsp60* promoter was removed from pMsGroEL1; pACEMsgroEL2 is a similar plasmid with groEL2 expression controlled by the inducible acetamidase promoter. Plasmid pMV261:KasA (Kremer et al., 2000b) is a derivative of vector pMV261 in which the *M. tuberculosis kasA* gene is fused to the *hsp60* promoter.

Construction of Mutants

The chromosomal copies of *groEL1*, *groEL2,* and *Smeg4308* were replaced in *M. smegmatis* mc^2155 using specialized transducing phages as described previously (Bardarov et al., 2002). In brief, 500–600 bp fragments upstream and downstream of the chromosomal gene were PCR-amplified using primers, and cognate upstream-downstream pairs were inserted into plasmid pYUB854 flanking its hygromycin resistance gene. Recombinant plasmids were then inserted into shuttle phasmid pAE87, phage particles recovered in *M. smegmatis*, and a high titer lysate used to transduce *M. smegmatis*. Hyg^R colonies were screened by Southern hybridization, and a clone containing a replacement of the gene with the hyg^R cassette was chosen for further studies. When making the *groEL2* allelic exchange substrate, the shuttle phasmid was also used to transduce *M. smegmatis* strains mc^2155pMsgroEL2 (a plasmid carrying the *M. smegmatis groEL2* gene) and mc^2155pACEMsgroEL2 (in which *groEL2* is fused to the inducible acetamidase promoter) and plated on 7H10 solid media containing hygromycin (mc^2155 and mc^2155pMsgroEL2) or on media containing hygromycin (150 μg/ml), acetamide (0.2%), and succinate (0.2%)

(mc^{2}155pACEMsgroEL2); construction of the Δ*kasB* strain is described elsewhere (Bhatt et al., 2005).

Purification of Native GroEL1 from *M. smegmatis*

Bacterial strains *M. smegmatis* mc^{2}155, *ΔgroEL1,* and mc^2 55pAlK6stop (Kim et al., 2003) were grown planktonically in 50 ml of biofilm media until an OD_{600} of 0.8 was achieved. The cells were harvested, washed once with cold PBS (4ºC), resuspended in 5 ml of binding buffer (50 mM Tris, pH 8.0, 150 mM NaCl, 5% vol./vol. glycerol), and disrupted by sonication (10 × 15 s). The lysates were centrifuged at 13,000 rpm for 20 min, and the supernatants were incubated with 2 ml preequilibrated Ni-Agarose for 60 min at 4ºC. The matrix was then washed with 40 ml of binding buffer before eluting with increasing concentrations of imidazole (20 mM and 75 mM) in 5 ml binding buffer. Samples containing 20 μl of eluate were analyzed by SDS-PAGE.

For comparative analysis of GroEL1 from planktonic and biofilm cultures, cells were grown either planktonically in 50 ml biofilm media or as biofilms in four plates. Cells from log phase planktonic and 4-day biofilm cultures were harvested and lysed as described above. About 15 mg of total cellular protein was subjected to 2 ml of preequilibrated Ni^{2+} agarose column and processed as above. All samples were eluted in 1 ml of elution buffer of which 20 μl was analyzed on the SDS-PAGE.

Proteomics

M. smegmatis mc^{2}155 and Δ*groEL1* strains were grown planktonically in biofilm medium at 37ºC to a density of OD_{600} of ~1.5. The cells were harvested, washed twice with NaHEPES (pH 8.0), and resuspended in 2 ml of lysis buffer (10 mM NaHEPES, pH 8.0, 7% urea, 4% CHAPS, 2 M thiourea, 10 mM DTT), followed by sonication with five pulses of 10 s each. The lysate was cleared by centrifugation at 13,000 rpm for 12 min at 4ºC. Approximately 170 μg of total protein of the supernatant was loaded on a hydrated 13 cm immobiline strip (Pharmacia, pH 4–7) and electrophoresed in an IPGphor system (Pharmacia) for a total of 72,000 Vhr for approximately 17 hr. After equilibration, strips were loaded and resolved in the second dimension through a 12% SDS-PAGE; proteins were identified by staining with colloidal Coomassie blue (Invitogen Inc.). Two spots that differed in intensity in two independent experiments were identified, one by N-terminal sequencing (N-AALSTGNGLPN), corresponding to residues 2–12 of *M. smegmatis* KasB (MSMEG1197), and the second by mass spectrometry as KasA.

Immunoblotting

M. smegmatis mc^{2}155, the Δ*groEL1* mutant, and complemented strains were grown in a 10 ml medium either in planktonic or in biofilm culture until a specified time. Cells were harvested, washed with Phosphate Buffered Saline (PBS), and resuspended in 500 μl of ice-cold 2D-PAGE lysis buffer, sonicated six times with 15 s pulse and centrifuged at 13,000 rpm for 20 min. Protein concentrations were determined using the BIO-RAD estimation kit (cat # 500-0006); 20 μg of total proteins per sample were loaded either on 2D-PAGE or 10% PAGE, blotted on PVDF membrane, and probed with a rat anti-KasA/KasB antibody raised against *M. tuberculosis* KasA protein (1:1000 dilution) (Kremer et al., 2002b). Horse radish peroxidase conjugated anti-rat serum was used as a secondary antibody (1:10000 dilution), and detection was carried out using the Western Lightening Reagent (Perkin Elmer) according to the manufacturer's instructions. For immunoblotting of biofilm samples on 1D PAGE, 2 μg of total protein per sample was loaded on 10% polyacrylamide gel and analyzed. Immunobloting of purified GroEL 1 (1 μg) or cell lysates (25 μg) resolved on a 10% SDS-PAGE were carried out using either polyclonal anti-*E. coli* GroEL rabbit serum (Stressgen Biotechnologies Inc.) used at 1: 3000 or monoclonal anti-BCG GroEL 2 mouse serum (Imgenex Inc.) used at 1:2000 dilution.

Mycolate Analysis

Twenty milliliter cultures of mc^{2}155, *ΔgroEL1,* and *ΔgroEL1* complemented strains were grown planktonically in a biofilm medium at 37ºC to OD_{600} 0.4. Twenty microcuries of ^{14}C-acetate (56.5 μCi/mM) were added and incubated for a further hour. Cells were harvested and treated overnight with 2 ml tetrabutylammonium hydroxide (40%) at 100ºC, followed by addition of 2 ml of dichloromethane and 200 μl of methyl iodide and mixing at room temperature for 1 hr. After centrifugation at 2,000 rpm for 10 min., the organic phase was washed once with 0.25N HCl and once with water before drying under vacuum. The powder was dissolved in 1 ml of dichloromethane and quantified by scintillation counting. Approximately 50,0000 cpm per sample was spotted on a silica-coated TLC plate and developed thrice in hexane:ethyle acetate (95:5, v/v), then twice in hexane:diethylether (85:15, v/v). The plate was exposed on Kodak XOMAT BMR film and viewed by autoradiography. For mycolate analysis of biofilm cells, the bacteria were grown as biofilm culture in the medium containing 20 μCi ^{14}C-acetate for 5 days.

For mass spectrometric analysis, unlabeled mycolates from planktonic and biofilm cultures were purified as described above. Total mycolates from each strain were analyzed by MALDI-MS (Voyager-DE, Applied Biosystems) by spotting the sample mixed with 2,5 dihydroxybenzoic acid as matrix and ionizing at a laser intensity setting of 3,500. Three hundred shots were averaged for each spectrum, and three independent spectra were obtained for each sample.

Supplemental Data

Supplemental Data include four figures and can be found with this article online at http://www.cell.com/cgi/content/full/123/5/861/DC1/.

ACKNOWLEDGMENTS

We thank Molly Scanlon for excellent technical support, John Hempel for N-terminal sequence analysis, Ashraf Ilamin in the University of Pittsburgh Proteomic Core laboratories for help with mass spectrometry, Tom Harper for photographic support, and Catherine Vilcheze for kindly providing the *inhA*^{ts} mutant. This work was supported from grant AI28927 to G.F.H. and AI26170 to W.R.J. L.K. is supported by a grant from the CNRS (ATIP "Microbiologie Fondamentale").

Received: April 1, 2005
Revised: July 27, 2005
Accepted: September 7, 2005
Published: December 1, 2005

REFERENCES

Baba, T., Kaneda, K., Kusunose, E., Kusunose, M., and Yano, I. (1989). Thermally adaptive changes of mycolic acids in Mycobacterium smegmatis. J. Biochem. (Tokyo) *106*, 81–86.

Bardarov, S., Bardarov Jr, S., Jr., Pavelka Jr, M.S., Jr., Sambandamurthy, V., Larsen, M., Tufariello, J., Chan, J., Hatfull, G., and Jacobs Jr, W.R. (2002). Specialized transduction: an efficient method for generating marked and unmarked targeted gene disruptions in Mycobacterium tuberculosis, M. bovis BCG and M. smegmatis. Microbiol. *148*, 3007–3017.

Barreiro, C., Gonzalez-Lavado, E., Brand, S., Tauch, A., and Martin, J.F. (2005). Heat shock proteome analysis of wild-type Corynebacterium glutamicum ATCC 13032 and a spontaneous mutant lacking GroEL1, a dispensable chaperone. J. Bacteriol. *187*, 884–889.

Beloin, C., and Ghigo, J.M. (2005). Finding gene-expression patterns in bacterial biofilms. Trends Microbiol. *13*, 16–19.

Bhatt, A., Kremer, L., Dai, A.Z., Sacchettini, J.C., and Jacobs, W.R., Jr. (2005). Conditional depletion of KasA, a key enzyme of mycolic acid biosynthesis, leads to mycobacterial cell death. J. Bacteriol. *187*, 7596–7606.

Braig, K., Otwinowski, Z., Hegde, R., Boisvert, D.C., Joachimiak, A., Horwich, A.L., and Sigler, P.B. (1994). The crystal structure of the bacterial chaperonin GroEL at 2.8 A. Nature *371*, 578–586.

Branda, S.S., Vik, S., Friedman, L., and Kolter, R. (2005). Biofilms: the matrix revisited. Trends Microbiol. *13*, 20–26.

Carter, G., Wu, M., Drummond, D.C., and Bermudez, L.E. (2003). Characterization of biofilm formation by clinical isolates of Mycobacterium avium. J. Med. Microbiol. *52*, 747–752.

Coates, A.R.M. (1996). Immunological aspects of chaperonins. In The chaperonins, R.A. Ellis, ed. (London, United Kingdom: Academic Press), pp. 267–296.

Dosanjh, N.S., Rawat, M., Chung, J.H., and Av-Gay, Y. (2005). Thiol specific oxidative stress response in Mycobacteria. FEMS Microbiol. Lett. *249*, 87–94.

Dubnau, E., Chan, J., Raynaud, C., Mohan, V.P., Laneelle, M.A., Yu, K., Quemard, A., Smith, I., and Daffe, M. (2000). Oxygenated mycolic acids are necessary for virulence of Mycobacterium tuberculosis in mice. Mol. Microbiol. *36*, 630–637.

Ewalt, K.L., Hendrick, J.P., Houry, W.A., and Hartl, F.U. (1997). In vivo observation of polypeptide flux through the bacterial chaperonin system. Cell *90*, 491–500.

Fayet, O., Ziegelhoffer, T., and Georgopoulos, C. (1989). The groES and groEL heat shock gene products of Escherichia coli are essential for bacterial growth at all temperatures. J. Bacteriol. *171*, 1379–1385.

Fisher, M.T. (1998). GroE chaperonin-assisted folding and assembly of dodecameric glutamine synthetase. Biochemistry (Mosc.) *63*, 382–398.

Fux, C.A., Costerton, J.W., Stewart, P.S., and Stoodley, P. (2005). Survival strategies of infectious biofilms. Trends Microbiol. *13*, 34–40.

Ghosh, P., Kim, A.I., and Hatfull, G.F. (2003). The orientation of mycobacteriophage Bxb1 integration is solely dependent on the central dinucleotide of attP and attB. Mol. Cell *12*, 1101–1111.

Glickman, M.S., Cox, J.S., and Jacobs, W.R., Jr. (2000). A novel mycolic acid cyclopropane synthetase is required for cording, persistence, and virulence of Mycobacterium tuberculosis. Mol. Cell *5*, 717–727.

Grimaud, R., and Toussaint, A. (1998). Assembly of both the head and tail of bacteriophage Mu is blocked in Escherichia coli groEL and groES mutants. J. Bacteriol. *180*, 1148–1153.

Guisbert, E., Herman, C., Lu, C.Z., and Gross, C.A. (2004). A chaperone network controls the heat shock response in E. coli. Genes Dev. *18*, 2812–2821.

Hall-Stoodley, L., and Stoodley, P. (2005). Biofilm formation and dispersal and the transmission of human pathogens. Trends Microbiol. *13*, 7–10.

Hall-Stoodley, L., Costerton, J.W., and Stoodley, P. (2004). Bacterial biofilms: from the natural environment to infectious diseases. Nat. Rev. Microbiol. *2*, 95–108.

Hartl, D.L., Lozovskaya, E.R., and Lawrence, J.G. (1992). Nonautonomous transposable elements in prokaryotes and eukaryotes. Genetica *86*, 47–53.

Hendrix, R.W., and Tsui, L. (1978). Role of the host in virus assembly: cloning of the Escherichia coli groE gene and identification of its protein product. Proc. Natl. Acad. Sci. USA *75*, 136–139.

Herman, C., and Gross, C.A. (2000). Heat stress. In Enclyclopedia of Microbiology, J. Lederberg, ed. (Academic Press), pp. 598–606.

Houry, W.A., Frishman, D., Eckerskorn, C., Lottspeich, F., and Hartl, F.U. (1999). Identification of in vivo substrates of the chaperonin GroEL. Nature *402*, 147–154.

Husson, R.N., and Young, R.A. (1987). Genes for the major protein antigens of Mycobacterium tuberculosis: the etiologic agents of tuberculosis and leprosy share an immunodominant antigen. Proc. Natl. Acad. Sci. USA *84*, 1679–1683.

Karlin, S., and Brocchieri, L. (2000). Heat shock protein 60 sequence comparisons: duplications, lateral transfer, and mitochondrial evolution. Proc. Natl. Acad. Sci. USA *97*, 11348–11353.

Kim, A., Ghosh, P., Aaron, M.A., Bibb, L.A., Jain, S., and Hatfull, G.F. (2003). Mycobacteriophage Bxb1 integrates into the *Mycobacterium smegmatis groEL1* gene. Mol. Microbiol. *50*, 463–473.

Kolter, R., and Losick, R. (1998). One for all and all for one. Science *280*, 226–227.

Kong, T.H., Coates, A.R., Butcher, P.D., Hickman, C.J., and Shinnick, T.M. (1993). Mycobacterium tuberculosis expresses two chaperonin-60 homologs. Proc. Natl. Acad. Sci. USA *90*, 2608–2612.

Kremer, K., Baulard, A., and Besra, G.S. (2000a). Genetics of mycolic acid biosynthesis. In Molecular Genetics of the Mycobacteria, G.F. Hatfull, and W.R. Jacobs, Jr., eds. (Washington, DC: ASM Press), pp. 173–190.

Kremer, L., Douglas, J.D., Baulard, A.R., Morehouse, C., Guy, M.R., Alland, D., Dover, L.G., Lakey, J.H., Jacobs, W.R., Jr., Brennan, P.J., et al. (2000b). Thiolactomycin and related analogues as novel anti-mycobacterial agents targeting KasA and KasB condensing enzymes in Mycobacterium tuberculosis. J. Biol. Chem. *275*, 16857–16864.

Kremer, L., Dover, L.G., Carrere, S., Nampoothiri, K.M., Lesjean, S., Brown, A.K., Brennan, P.J., Minnikin, D.E., Locht, C., and Besra, G.S. (2002a). Mycolic acid biosynthesis and enzymic characterization of the beta-ketoacyl-ACP synthase A-condensing enzyme from Mycobacterium tuberculosis. Biochem. J. *364*, 423–430.

Kremer, L., Guerardel, Y., Gurcha, S.S., Locht, C., and Besra, G.S. (2002b). Temperature-induced changes in the cell-wall components of Mycobacterium thermoresistibile. Microbiol. *148*, 3145–3154.

Kremer, L., Dover, L.G., Morbidoni, H.R., Vilcheze, C., Maughan, W.N., Baulard, A., Tu, S.C., Honore, N., Deretic, V., Sacchettini, J.C., et al. (2003). Inhibition of InhA activity, but not KasA activity, induces formation of a KasA-containing complex in mycobacteria. J. Biol. Chem. *278*, 20547–20554.

Kressel, A.B., and Kidd, F. (2001). Pseudo-outbreak of Mycobacterium chelonae and Methylobacterium mesophilicum caused by contamination of an automated endoscopy washer. Infect. Control Hosp. Epidemiol. *22*, 414–418.

Laval, F., Laneelle, M.A., Deon, C., Monsarrat, B., and Daffe, M. (2001). Accurate molecular mass determination of mycolic acids by MALDI-TOF mass spectrometry. Anal. Chem. *73*, 4537–4544.

Lewis, J.A., and Hatfull, G.F. (2000). Identification and characterization of mycobacteriophage L5 excisionase. Mol. Microbiol. *35*, 350–360.

Lewthwaite, J.C., Coates, A.R., Tormay, P., Singh, M., Mascagni, P., Poole, S., Roberts, M., Sharp, L., and Henderson, B. (2001). Mycobacterium tuberculosis chaperonin 60.1 is a more potent cytokine stimulator than chaperonin 60.2 (Hsp 65) and contains a CD14-binding domain. Infect. Immun. *69*, 7349–7355.

Maguire, M., Coates, A.R., and Henderson, B. (2002). Chaperonin 60 unfolds its secrets of cellular communication. Cell Stress Chaperones *7*, 317–329.

Marsollier, L., Severin, T., Aubry, J., Merritt, R.W., Saint Andre, J.P., Legras, P., Manceau, A.L., Chauty, A., Carbonnelle, B., and Cole, S.T. (2004a). Aquatic snails, passive hosts of Mycobacterium ulcerans. Appl. Environ. Microbiol. *70*, 6296–6298.

Marsollier, L., Stinear, T., Aubry, J., Saint Andre, J.P., Robert, R., Legras, P., Manceau, A.L., Audrain, C., Bourdon, S., Kouakou, H., and Carbonnelle, B. (2004b). Aquatic plants stimulate the growth of and biofilm formation by Mycobacterium ulcerans in axenic culture and harbor these bacteria in the environment. Appl. Environ. Microbiol. *70*, 1097–1103.

Marsollier, L., Aubry, J., Coutanceau, E., Andre, J.P., Small, P.L., Milon, G., Legras, P., Guadagnini, S., Carbonnelle, B., and Cole, S.T. (2005). Colonization of the salivary glands of Naucoris cimicoides by Mycobacterium ulcerans requires host plasmatocytes and a macrolide toxin, mycolactone. Cell. Microbiol. *7*, 935–943.

Mdluli, K., Slayden, R.A., Zhu, Y., Ramaswamy, S., Pan, X., Mead, D., Crane, D.D., Musser, J.M., and Barry, C.E., 3rd. (1998). Inhibition of a Mycobacterium tuberculosis beta-ketoacyl ACP synthase by isoniazid. Science *280*, 1607–1610.

Mediavilla, J., Jain, S., Kriakov, J., Ford, M.E., Duda, R.L., Jacobs, W.R., Jr., Hendrix, R.W., and Hatfull, G.F. (2000). Genome organization and characterization of mycobacteriophage Bxb1. Mol. Microbiol. *38*, 955–970.

Miller, M.B., and Bassler, B.L. (2001). Quorum sensing in bacteria. Annu. Rev. Microbiol. *55*, 165–199.

Monahan, I.M., Betts, J., Banerjee, D.K., and Butcher, P.D. (2001). Differential expression of mycobacterial proteins following phagocytosis by macrophages. Microbiol. *147*, 459–471.

Nyka, W. (1974). Studies on the effect of starvation on mycobacteria. Infect. Immun. *9*, 843–850.

O'Toole, G.A., Pratt, L.A., Watnick, P.I., Newman, D.K., Weaver, V.B., and Kolter, R. (1999). Genetic approaches to study of biofilms. Methods Enzymol. *310*, 91–109.

Ogawa, J., and Long, S.R. (1995). The Rhizobium meliloti groELc locus is required for regulation of early nod genes by the transcription activator NodD. Genes Dev. *9*, 714–729.

Orme, I.M., Roberts, A.D., Griffin, J.P., and Abrams, J.S. (1993). Cytokine secretion by CD4 T lymphocytes acquired in response to Mycobacterium tuberculosis infection. J. Immunol. *151*, 518–525.

Primm, T.P., Lucero, C.A., and Falkinham, J.O., 3rd. (2004). Health impacts of environmental mycobacteria. Clin. Microbiol. Rev. *17*, 98–106.

Recht, J., and Kolter, R. (2001). Glycopeptidolipid acetylation affects sliding motility and biofilm formation in Mycobacterium smegmatis. J. Bacteriol. *183*, 5718–5724.

Recht, J., Martinez, A., Torello, S., and Kolter, R. (2000). Genetic analysis of sliding motility in Mycobacterium smegmatis. J. Bacteriol. *182*, 4348–4351.

Reguera, G., and Kolter, R. (2005). Virulence and the environment: a novel role for Vibrio cholerae toxin-coregulated pili in biofilm formation on chitin. J. Bacteriol. *187*, 3551–3555.

Rose, L., Kaufmann, S.H., and Daugelat, S. (2004). Involvement of Mycobacterium smegmatis undecaprenyl phosphokinase in biofilm and smegma formation. Microbes Infect. *6*, 965–971.

Saibil, H. (2000). Molecular chaperones: containers and surfaces for folding, stabilising or unfolding proteins. Curr. Opin. Struct. Biol. *10*, 251–258.

Schaeffer, M.L., Agnihotri, G., Volker, C., Kallender, H., Brennan, P.J., and Lonsdale, J.T. (2001). Purification and biochemical characterization of the Mycobacterium tuberculosis beta-ketoacyl-acyl carrier protein synthases KasA and KasB. J. Biol. Chem. *276*, 47029–47037.

Schulze-Robbecke, R., Janning, B., and Fischeder, R. (1992). Occurrence of mycobacteria in biofilm samples. Tuber. Lung Dis. *73*, 141–144.

Sigler, P.B., Xu, Z., Rye, H.S., Burston, S.G., Fenton, W.A., and Horwich, A.L. (1998). Structure and function in GroEL-mediated protein folding. Annu. Rev. Biochem. *67*, 581–608.

Singh, P.K., Parsek, M.R., Greenberg, E.P., and Welsh, M.J. (2002). A component of innate immunity prevents bacterial biofilm development. Nature *417*, 552–555.

Slayden, R.A., and Barry, C.E., 3rd. (2002). The role of KasA and KasB in the biosynthesis of meromycolic acids and isoniazid resistance in Mycobacterium tuberculosis. Tuberculosis (Edinb.) *82*, 149–160.

Smeulders, M.J., Keer, J., Speight, R.A., and Williams, H.D. (1999). Adaptation of Mycobacterium smegmatis to stationary phase. J. Bacteriol. *181*, 270–283.

Stewart, G.R., Wernisch, L., Stabler, R., Mangan, J.A., Hinds, J., Laing, K.G., Young, D.B., and Butcher, P.D. (2002). Dissection of the heat-shock response in Mycobacterium tuberculosis using mutants and microarrays. Microbiol. *148*, 3129–3138.

Taneja, B., and Mande, S.C. (2001). Metal ions modulate the plastic nature of Mycobacterium tuberculosis chaperonin-10. Protein Eng. *14*, 391–395.

Teng, R., and Dick, T. (2003). Isoniazid resistance of exponentially growing Mycobacterium smegmatis biofilm culture. FEMS Microbiol. Lett. *227*, 171–174.

Veyron-Churlet, R., Guerrini, O., Mourey, L., Daffe, M., and Zerbib, D. (2004). Protein-protein interactions within the Fatty Acid Synthase-II system of Mycobacterium tuberculosis are essential for mycobacterial viability. Mol. Microbiol. *54*, 1161–1172.

Vilcheze, C., Morbidoni, H.R., Weisbrod, T.R., Iwamoto, H., Kuo, M., Sacchettini, J.C., and Jacobs, W.R., Jr. (2000). Inactivation of the inhA-encoded fatty acid synthase II (FASII) enoyl- acyl carrier protein reductase induces accumulation of the FASI end products and cell lysis of Mycobacterium smegmatis. J. Bacteriol. *182*, 4059–4067.

Xu, Z., Horwich, A.L., and Sigler, P.B. (1997). The crystal structure of the asymmetric GroEL-GroES-(ADP)7 chaperonin complex. Nature *388*, 741–750.

Young, D., Lathigra, R., Hendrix, R., Sweetser, D., and Young, R.A. (1988). Stress proteins are immune targets in leprosy and tuberculosis. Proc. Natl. Acad. Sci. USA *85*, 4267–4270.

Yuan, Y., Zhu, Y., Crane, D.D., and Barry, C.E., 3rd. (1998). The effect of oxygenated mycolic acid composition on cell wall function and macrophage growth in Mycobacterium tuberculosis. Mol. Microbiol. *29*, 1449–1458.